The formation and disordered degradation of neutrophil extracellular traps in necrotizing lesions of anti-neutrophil cytoplasmic antibody-associated vasculitis

Sakiko Masuda[1,2], Mayu Nonokawa[1], Emika Futamata[1], Yuka Nishibata[1], Sari Iwasaki[3], Takahiro Tsuji[3], Yutaka Hatanaka[4], Daigo Nakazawa[2], Satoshi Tanaka[5], Utano Tomaru[6], Tamihiro Kawakami[7,*], Tatsuya Atsumi[2], Akihiro Ishizu[1]

[1]Department of Medical Laboratory Science, Faculty of Health Sciences, Hokkaido University, Sapporo, Japan

[2]Department of Rheumatology, Endocrinology and Nephrology, Faculty of Medicine and Graduate School of Medicine, Hokkaido University, Sapporo, Japan

[3]Department of Pathology, Sapporo City Hospital, Sapporo, Japan

[4]Research Division of Genome Companion Diagnostics, Hokkaido University Hospital, Sapporo, Japan

[5]Center for Cause of Death Investigation, Graduate School of Medicine, Hokkaido University, Sapporo, Japan

[6]Department of Pathology, Faculty of Medicine and Graduate School of Medicine, Hokkaido University, Sapporo, Japan

[7]Department of Dermatology, St. Marianna University School of Medicine, Kawasaki, Japan

*Currently in the Department of Dermatology, Tohoku Medical and Pharmaceutical University, Sendai, Japan

Competing interests: The authors declare no conflict of interest.

Correspondence: Prof. Akihiro Ishizu, Faculty of Health Sciences, Hokkaido University, Kita-12, Nishi-5, Kita-ku, Sapporo 060-0812, Japan; aishizu@med.hokudai.ac.jp

Funding: This study was supported by a grant for Japan Research Committee of the Ministry of Health, Labour, and Welfare for Intractable Vasculitis (A.I.) and by a grant from the Japan Agency for Medical Research and Development (grant number 15ek0109121) (A.I.).

Abbreviations

AAV: ANCA-associated vasculitis; ANCA: anti-neutrophil cytoplasmic antibody; CA: cutaneous arteritis; Cit H3: citrullinated histone 3; CGD: chronic granulomatous disease; DAPI: 4′,6-diamidino-2-phenylindole; EGPA: eosinophilic granulomatosis with polyangiitis; ERK: Extracellular signal-regulated kinase; FFPE: formalin-fixed paraffin-embedded; GCA: giant cell arteritis; GPA: granulomatosis with polyangiitis; HE: hematoxylin and eosin; MEK: Mitogen-activated protein kinase/ERK kinase; MLKL: Mixed lineage kinase domain-like pseudokinase; MPA: microscopic polyangiitis; MPO: myeloperoxidase; NET: neutrophil extracellular trap; PAD4: peptidylarginine deiminase 4; PAN: polyarteritis nodosa; PMA: phorbol myristate acetate; RIPK: Receptor-interacting serine/threonine-protein kinase; PR3: proteinase 3; SH: simple hematoxylin

Abstract

Anti-neutrophil cytoplasmic antibody (ANCA)-associated vasculitis (AAV) is characterized by production of ANCAs and systemic necrotizing vasculitis in small vessels. Disordered regulation of neutrophil extracellular traps (NETs) is critically involved in the pathogenesis of AAV. NETs are web-like DNA decorated with antimicrobial proteins; they are extruded from activated neutrophils. The principal degradation factor of NETs *in vivo* is DNase I; however, NETs resistant to DNase I can persist in tissues and lead to the production of ANCAs. Deposition of NETs has been demonstrated in glomerular crescents and necrotizing vasculitis in AAV. Here, we first examined the amount of NETs in formalin-fixed paraffin-embedded tissue sections and compared the results for AAV with the results for diseases that should be distinguished from AAV. We determined that NETs were more abundant in necrotizing vasculitis of AAV than in non-ANCA-associated vasculitis, or in granulomatous angiitis. We next focused on pulmonary granulomas in AAV and non-ANCA-associated diseases. The amount of NETs was significantly greater in necrotizing granulomas of AAV than in granulomas of sarcoidosis without necrosis. Although NETs were formed in necrotizing granulomas of tuberculosis equivalently to those formed in AAV, they were more susceptible to degradation by DNase I than were NETs in AAV. The formation and disordered degradation of NETs in necrotizing lesions are characteristics of AAV, and are possibly related to its pathogenesis.

Key words: NETs, ANCA, AAV, DNase I

Introduction

Anti-neutrophil cytoplasmic antibody (ANCA)-associated vasculitis (AAV) includes microscopic polyangiitis (MPA), granulomatosis with polyangiitis (GPA), and eosinophilic granulomatosis with polyangiitis (EGPA) (1). AAV is characterized by production of ANCAs and systemic necrotizing vasculitis in small vessels. In addition, necrotizing granulomas in the lung are typically observed in GPA. ANCAs are known as pathogenic autoantibodies in AAV and the major target antigens are myeloperoxidase (MPO) and proteinase 3 (PR3). ANCAs bind to the antigens and simultaneously bridge the antigens and bystander Fcγ receptors on neutrophils primed by pro-inflammatory cytokines, such as TNF-α. Consequently, the neutrophils are activated to release reactive oxygen species and lytic enzymes, in turn contributing to the development of small vessel vasculitis. This ANCA-cytokine sequence is pivotal for understanding the pathogenesis of AAV (2).

In 2004, Brinkmann et al. reported that phorbol myristate acetate (PMA) stimulates neutrophils to extrude a decondensed DNA that forms an extracellular web-like structure decorated with antimicrobial proteins, including MPO, PR3, and histones (3). These substances, termed neutrophil extracellular traps (NETs), can capture and kill microbes. Patients with chronic granulomatous disease (CGD) who fail to generate NETs are susceptible to diverse bacterial and fungal infections. In contrast, restoration of NET formation in CGD by gene therapy results in resistance to such infections (4). Thus, NET formation is an important event of innate immunity. However, some components of NETs, including MPO, PR3, and histones, have adverse effects on the host, such as cytotoxicity to vascular endothelial cells and thrombogenicity (5).

Kessenbrock et al. were the first to report the relationship of AAV and NETs (6). They demonstrated the presence of NETs in glomerular crescents of AAV patients

and that ANCAs could induce release of NETs from neutrophils primed by TNF-α. It is currently considered that NETs extruded from activated neutrophils are implicated in vascular endothelial cell injury in the ANCA-cytokine sequence (7).

Because of the adverse aspects to the host, NETs are strictly regulated *in vivo*. The most important NET degradation factor is serum DNase I (8). We have demonstrated that NETs resistant to degradation by DNase I are critically involved in the production of ANCAs, especially MPO-ANCAs (9). We have also demonstrated that sera of MPA patients have low DNase I activity and a correspondingly decreased ability to degrade NETs (10).

PMA-stimulated neutrophils undergo cell death accompanied by NET formation (11). Since the characteristics of this type of cell death resemble neither typical necrosis nor apoptosis, Steinberg et al. coined the term NETosis to describe neutrophilic cell death with NET formation (12). NETosis induced by PMA requires activation of the Raf-MEK-ERK (Raf-Mitogen-activated protein kinase/ERK kinase-Extracellular signal-regulated kinase) pathway and RIPK1-RIPK3-MLKL (Receptor-interacting serine/threonine-protein kinase 1-RIPK3-Mixed lineage kinase domain-like pseudokinase) pathway (13, 14). In this process, peptidylarginine deiminase 4 (PAD4)-dependent citrullination of histones induces decondensation of DNA resulting in a mixture of DNA and bactericidal proteins originally contained in intracytoplasmic granules (15). Thereafter, these substances are extruded from the ruptured plasma membrane of neutrophils. Thus, citrullinated histones can be reliable markers of NETs.

The presence of NETs has been shown in glomerular crescents (6), deep vein thromboses (16, 17), and necrotizing vasculitis (18) in AAV. In this study, we examined the amounts of NETs in formalin-fixed paraffin-embedded (FFPE) tissue sections and compared the results for AAV with the results for diseases that should be distinguished

from AAV.

Materials and Methods

Clots containing NETs

Human peripheral blood neutrophils were obtained from healthy volunteers by density centrifugation using Polymorphprep (Axis-Shield, Dundee, Scotland). The neutrophils were suspended in RPMI 1640 medium containing 5% fetal bovine serum in a polypropylene tube (1×10^6/ml) and subsequently exposed to 100 nM PMA (Sigma-Aldrich, St. Louis, MO) for 4 h at 37 ºC. During incubation, the tube was periodically gently shaken. Thereafter, the samples were fixed with 10% formalin and a clot was generated by the sodium alginate method (19). The clot was embedded in paraffin wax for making a FFPE specimen. This study was conducted with the permission of the Ethical Committee of the Faculty of Health Sciences, Hokkaido University (Permission No. 17-85 and 18-61).

FFPE tissue sections

Tissue samples from 8 patients with AAV (3 with MPA, 4 with GPA, and 1 with EGPA) were used. For controls, tissue samples from 10 patients with non-ANCA-associated vasculitis (3 with polyarteritis nodosa [PAN], 2 with cutaneous arteritis [CA], and 5 with giant cell arteritis [GCA]), and 10 patients with non-vasculitic diseases (5 with tuberculosis and 5 with sarcoidosis) were used. These samples were obtained by biopsy, surgery, or autopsy, and were fixed with 10% formalin and embedded in paraffin wax. Details of the FFPE specimens used in this study are shown in **Table 1**.

Immunofluorescent staining

FFPE specimens were sliced into 4 μm sections and then deparaffinized with xylene. After antigen retrieval in an autoclave (at 121 ºC for 20 min) with Tris-EDTA buffer (pH 9.0), the sections were soaked in Protein Block Serum-free (Dako, Glostrup, Denmark) for 10 min at room temperature to inhibit non-specific binding of antibodies. Primary antibodies used were anti-citrullinated histone 3 (Cit H3; rabbit polyclonal, 1:100 dilution; Abcam, Eugene, OR) and anti-CD15 (mouse IgM, ready-to-use; Dako). After incubation with primary antibodies for 1 h at room temperature, the sections were washed with PBS. Secondary antibodies used were Alexa Fluor 594-conjugated goat anti-rabbit IgG H&L at 1:500 dilution (Abcam) and Alexa Fluor 488-conjugated goat anti-mouse IgM at 1:500 dilution (Invitrogen, Carlsbad, CA). After incubation with secondary antibodies for 1 h at room temperature, the sections were washed with PBS and then mounted with a mounting solution containing 4′,6-diamidino-2-phenylindole (DAPI) (Vector Laboratories, Burlingame, CA). The slides were observed under a fluorescence microscope.

Hematoxylin staining with or without eosin staining

FFPE sections were deparaffinized with xylene and then allowed to react with hematoxylin solution. After washing the surplus stain out of the cytoplasm with 1% hydrochloric acid in 70% alcohol, the sections were allowed to react with or without eosin solution. The former is conventional hematoxylin and eosin (HE) staining. We named the latter simple hematoxylin (SH) staining.

DNase I treatment

FFPE clot sections of PMA-treated neutrophils were deparaffinized with xylene and then subjected to antigen retrieval in an autoclave (at 121 ºC for 20 min) with citrate buffer (pH 6.0). Thereafter, the sections were allowed to react with 1 or 10

U/ml DNase I (Invitrogen) for 1 h at 37 ºC. After washing with PBS, the sections were subjected to immunofluorescent staining for Cit H3 and SH staining. FFPE tissue sections of AAV and tuberculosis were deparaffinized with xylene and then treated by DNase I similarly. After washing with PBS, the sections were mounted using the DAPI-containing solution or subjected to immunofluorescent staining for Cit H3/CD15 and SH staining.

Image analysis

Image analysis was performed using ImageJ software. The area occupied by NETs within the lesion (%) was calculated as follows: [(area of NETs determined as Cit H3-positive area) / (lesion area determined by HE staining)] × 100. The percentage of NETs remaining after DNase I treatment [NETs residual rate (%)] was calculated by using the mean brightness of the DAPI images or SH images as follows: [(mean brightness after DNase I treatment) / (mean brightness before DNase I treatment)] × 100. When multiple lesions were present in a specimen, we calculated the mean value of the 'Area occupied by NETs within the lesion (%)' and the 'NETs residual rate (%).'

Statistical analysis

The Mann-Whitney *U*-test was applied for comparison of two non-parametric groups. A *p*-value of less than 0.05 was regarded as statistically significant.

Results

Visualization of NETs in FFPE sections

Immunofluorescent staining for Cit H3 is the method that has been generally applied to visualize NETs (20). In this study, SH staining was additionally performed to observe NETs by light microscopy. Peripheral blood neutrophils stimulated by 100 nM PMA were employed for making FFPE clot specimens. Sections from the FFPE specimens were subjected to immunofluorescent staining for Cit H3 and SH staining. In immunofluorescent staining, Cit H3-positive DAPI-positive substances were determined as NETs (**Figure 1A**). Based on the finding that most of the Cit H3-positive area was also DAPI-positive, the Cit H3-positive area was regarded as the area of NETs for the remainder of this study. Since hematoxylin can stain nucleic acid (21), we next conducted SH staining to visualize NETs in the FFPE sections. As expected, NETs were also identified as hematoxylin-stained substances around neutrophils (**Figure 1B**).

It has been demonstrated that NETs induced by PMA are digested by DNase I in the cell culture system (8). Thus, we examined whether PMA-induced NETs in FFPE sections could also be digested by DNase I similarly to that under the cell culture conditions. Our preliminary experiments indicated that 10 U/ml (but not 1 U/ml) DNase I exposure for 1 h at 37 ºC could effectively digest the PMA-induced NETs in FFPE sections. DNase I treatment (10 U/ml, for 1 h, at 37 ºC) resulted in the digestion of NETs in FFPE sections (**Figures 1C and 1D**). We also noted at the same time that Cit H3 was not removed completely by the DNase I treatment, whereas almost all of the extracellular DNA stained by DAPI and hematoxylin was digested by DNase I.

Presence of NETs in vasculitis

We divided the vasculitides into three groups—necrotizing vasculitis in AAV, necrotizing vasculitis in non-ANCA-associated vasculitis, and granulomatous angiitis—focusing on the presence of ANCAs and fibrinoid necrosis, and then compared the amounts of NETs in each of the groups. Cit H3-positive substances were present around fibrinoid necrosis in vasculitic lesions of AAV (MPA: **Figures 2A** and **2B**; EGPA: **Figures 2C** and **2D**). The distribution of CD15-positive cells (regarded as neutrophils) was consistent with the localization of Cit H3-positive substances in MPA, but not in EGPA. A characteristic of EGPA is abundant infiltration of eosinophils around fibrinoid necrosis in vasculitic lesions. Since eosinophils can release extracellular traps (22), the Cit H3-positive substances in EGPA are thought to be derived from eosinophils.

Interestingly, the amount of NETs was much smaller in necrotizing vasculitis of non-ANCA-associated vasculitis (CA: **Figures 2E** and **2F**). NETs were hardly detected in granulomatous angiitis of GCA (**Figures 2G** and **2H**). The area occupied by NETs within the lesion was significantly greater in necrotizing vasculitis of AAV than in non-ANCA-associated vasculitis or granulomatous angiitis (**Figure 2I**). These findings are consistent with the concept that ANCA-induced NETs are involved in the pathogenesis of necrotizing vasculitis in AAV (7). It should be noted that the 'Area occupied by NETs within the lesion (%)' varied among patients with AAV. We considered that this variance might be associated with the diverse phases of vasculitis usually observed in a patient with AAV (1).

Presence of NETs in pulmonary granulomas

Next, we determined the presence of NETs in pulmonary granulomas. Pulmonary granulomas were divided into three groups—necrotizing granulomas in AAV, necrotizing granulomas in non-ANCA-associated diseases, and granulomas without necrosis in non-ANCA-associated diseases—focusing on the presence of ANCAs and

necrosis. Abundant NETs were present in necrotizing granulomas in the lung tissues of patients with GPA (**Figures 3A** and **3B**) and tuberculosis (**Figures 3C** and **3D**) but not in pulmonary granulomas of sarcoidosis without necrosis (**Figures 3E** and **3F**). The distribution of CD15-positive cells (regarded as neutrophils) was consistent with the localization of NETs in both GPA and tuberculosis. The area occupied by NETs within the lesion was significantly greater in GPA and tuberculosis than in sarcoidosis (**Figure 3G**).

Disordered degradation of NETs in AAV

NETs were present in necrotizing granulomas in the lung tissues of patients with GPA and tuberculosis. These findings are consistent with the fact that both ANCAs and mycobacterium infection can induce NETs (6, 23, 24). Since it is suspected that NETs resistant to DNase I are associated with ANCA production (16), we examined DNase I resistance of NETs in GPA and tuberculosis. For this purpose, FFPE lung tissue sections of GPA and tuberculosis treated with or without DNase I (10 U/ml, for 1 h, at 37 ºC) were subjected to DAPI staining and SH staining. Since NETs can be stained by a single dye in these methods, either method is expected to be suitable for evaluation of the degradation of NETs by DNase I. Our results demonstrated that NETs in necrotizing granulomas in the lung tissues of GPA were not easily digested by DNase I compared with those of tuberculosis (GPA: **Figures 4A-4D**; tuberculosis: **Figures 4E-4H**; DAPI staining: **Figures 4A, 4B, 4E, 4F,** and **4I**; SH staining: **Figures 4C, 4D, 4G, 4H,** and **4J**). In contrary, Cit H3 remained even after the DNase I treatment in necrotizing granulomas of tuberculosis (Figure S1). We further examined if NETs in necrotizing vasculitic lesions of MPA were digested by DNase I. Our results suggested that they were also resistant to DNase I (Figure S2).

Discussion

In this study, we demonstrated the following: 1) NETs can be detected in FFPE sections by SH staining as well as by immunofluorescent staining for Cit H3, and NETs in FFPE sections can be digested by DNase I in a manner similar to that under cell culture conditions, 2) NETs are present specifically in vasculitic lesions of AAV, and 3) DNase I-resistant NETs are present in necrotizing lesions of AAV (Tables 2 and 3).

Concerning the first issue, detection of NETs in human samples is still challenging (20). Currently, immunofluorescent staining for NET components, such as Cit H3, is regarded as the most reliable method for detecting NETs in tissue samples; however, this method requires working in the dark, which is somewhat of a burden for investigators. SH staining can be helpful in that specimens are observed under a light microscope. In addition, to the best of our knowledge, this study is the first to demonstrate that NETs in FFPE sections can be digested by DNase I treatment. Although DNA in the nuclei of cells in FFPE sections can also be digested by DNase I, extracellular DNA of NETs was more susceptible to the treatment (10 U/ml of DNase I, for 1 h, at 37 ºC) than was intranuclear DNA. The susceptibility to DNase I could be different for extracellular DNA and intranuclear DNA. As described below, DNase I resistance appears to be one of the characteristics of NETs in AAV. Since NETs themselves are formed in healthy individuals when necessary, the DNase I digestion test can be useful to distinguish ANCA-related NETs from non-ANCA-related NETs.

Secondly, we determined that NETs were more abundant in necrotizing vasculitis of AAV than in non-ANCA-associated vasculitis, such as PAN and CA, or in granulomatous angiitis of GCA. NETs were present around fibrinoid necrosis in the affected vessels. Yoshida et al. also reported that Cit H3 was located around fibrinoid

necrosis in necrotizing interlobular arteries of the kidney (18). Moreover, we have noted the presence of NETs around small vessels without fibrinoid necrosis in MPA patients (data not shown). Recent studies have demonstrated that ANCA-induced NETs possess cytotoxic activity towards vascular endothelial cells (25). Collectively, these findings suggest that NETs induced by ANCAs are responsible for the formation of fibrinoid necrosis in the vasculitic lesions of AAV.

Lastly, we demonstrated that NETs were present in necrotizing pulmonary granulomas of GPA and tuberculosis but not in pulmonary granulomas of sarcoidosis without necrosis. This is the first evidence of the presence of NETs in necrotizing granulomas of GPA. NETs were located in the necrotic lesions but not in granulation tissues surrounding the necrosis. This is inconsistent with the finding of vasculitic lesions; however, the reason has not been revealed. NETs are also present in necrotizing granulomas in the lungs of patients with tuberculosis. *Mycobacterium tuberculosis* is phagocytosed by neutrophils and alveolar macrophages, and the neutrophils release NETs to prevent the spread of *Mycobacterium tuberculosis* (24). Interestingly, NETs formed in the necrotizing granulomas of GPA were not easily degraded by DNase I compared with NETs formed in tuberculosis. We have demonstrated that DNase I-resistant NETs induced by the anti-thyroid drug propylthiouracil could induce the production of MPO-ANCAs and subsequent development of AAV *in vivo* (9). These findings collectively suggest that DNase I-resistant NETs in necrotizing granulomas of GPA can be a source of ANCA antigens. We currently cannot demonstrate the mechanism underlying how NETs acquire resistance to DNase I in AAV. However, this issue seems to be very important; thus, we are now carrying out a comparative transcriptome analysis between NETs in AAV and in non-ANCA-associated vasculitis.

In conclusion, the collective findings suggest that the formation and disordered degradation of NETs in necrotizing lesions are characteristics of AAV, and

are possibly related to its pathogenesis.

Authors' contributions

S.M., S.I., T.T., Y.H., T.K., U.T., and A.I. designed the study. S.M., M.N., E.F., and Y.N. performed the experiments. S.M., D.N., S.T., U.T., T.A., and A.I. analyzed the data. S.M., U.T., and A.I. wrote the manuscript.

References

1. Jennette JC, Falk RJ, Bacon PA, Basu N, Cid MC, Ferrario F, Flores-Suarez LF, Gross WL, Guillevin L, Hagen EC, Hoffman GS, Jayne DR, Kallenberg CG, Lamprecht P, Langford CA, Luqmani RA, Mahr AD, Matteson EL, Merkel PA, Ozen S, Pusey CD, Rasmussen N, Rees AJ, Scott DG, Specks U, Stone JH, Takahashi K, Watts RA: 2012 revised International Chapel Hill Consensus Conference Nomenclature of Vasculitides. Arthritis Rheum 2013, 65:1-11.

2. Csernok E: Anti-neutrophil cytoplasmic antibodies and pathogenesis of small vessel vasculitides. Autoimmun Rev 2003, 2:158-164.

3. Brinkmann V, Reichard U, Goosmann C, Fauler B, Uhlemann Y, Weiss DS, Weinrauch Y, Zychlinsky A: Neutrophil extracellular traps kill bacteria. Science 2004, 303:1532-1535.

4. Bianchi M, Hakkim A, Brinkmann V, Siler U, Seger RA, Zychlinsky A, Reichenbach J: Restoration of NET formation by gene therapy in CGD controls aspergillosis. Blood 2009, 114:2619-2622.

5. Doring Y, Weber C, Soehnlein O: Footprints of neutrophil extracellular traps as predictors of cardiovascular risk. Arterioscler Thromb Vasc Biol 2013, 33:1735-1736.

6. Kessenbrock K, Krumbholz M, Schonermarck U, Back W, Gross WL, Werb Z, Grone HJ, Brinkmann V, Jenne DE: Netting neutrophils in autoimmune small-vessel vasculitis. Nat Med 2009, 15:623-625.

7. Jennette JC, Falk RJ: Pathogenesis of antineutrophil cytoplasmic autoantibody-mediated disease. Nat Rev Rheumatol 2014, 10:463-473.

8. Hakkim A, Furnrohr BG, Amann K, Laube B, Abed UA, Brinkmann V, Herrmann M, Voll RE, Zychlinsky A: Impairment of neutrophil extracellular trap degradation is associated with lupus nephritis. Proc Natl Acad Sci USA 2010, 107:9813-9818.

9. Nakazawa D, Tomaru U, Suzuki A, Masuda S, Hasegawa R, Kobayashi T, Nishio S, Kasahara M, Ishizu A: Abnormal conformation and impaired degradation of propylthiouracil-induced neutrophil extracellular traps: implications of disordered neutrophil extracellular traps in a rat model of myeloperoxidase antineutrophil cytoplasmic antibody-associated vasculitis. Arthritis Rheum 2012, 64:3779-3787.

10. Nakazawa D, Shida H, Tomaru U, Yoshida M, Nishio S, Atsumi T, Ishizu A: Enhanced formation and disordered regulation of NETs in myeloperoxidase-ANCA-associated microscopic polyangiitis. J Am Soc Nephrol 2014, 25:990-997.

11. Fuchs TA, Abed U, Goosmann C, Hurwitz R, Schulze I, Wahn V, Weinrauch Y, Brinkmann V, Zychlinsky A: Novel cell death program leads to neutrophil extracellular traps. J Cell Biol 2007, 176:231-241.

12. Steinberg BE, Grinstein S: Unconventional roles of the NADPH oxidase: signaling, ion homeostasis, and cell death. Sci STKE 2007, 2007:pe11.

13. Hakkim A, Fuchs TA, Martinez NE, Hess S, Prinz H, Zychlinsky A Waldmann H: Activation of the Raf-MEK-ERK pathway is required for neutrophil extracellular trap formation. Nat Chem Biol 2011, 7:75-77.

14. Desai J, Kumar SV, Mulay SR, Konrad L, Romoli S, Schauer C, Herrmann M, Bilyy R, Muller S, Popper B, Nakazawa D, Weidenbusch M, Thomasova D, Krautwald S, Linkermann A, Anders HJ: PMA and crystal-induced neutrophil extracellular trap formation involves RIPK1-RIPK3-MLKL signaling. Eur J Immunol 2016, 46:223-229.

15. Li P, Li M, Lindberg MR, Kennett MJ, Xiong N, Wang Y: PAD4 is essential for antibacterial innate immunity mediated by neutrophil extracellular traps. J Exp Med 2010, 207:1853-1862.

16. Nakazawa D, Tomaru U, Yamamoto C, Jodo S, Ishizu A: Abundant neutrophil extracellular traps in thrombus of patient with microscopic polyangiitis. Front Immunol 2012, 3:333.

17. Imamoto T, Nakazawa D, Shida H, Suzuki A, Otsuka N, Tomaru U, Ishizu A: Possible linkage between microscopic polyangiitis and thrombosis via neutrophil extracellular traps. Clin Exp Rheumatol 2014, 32:149-150.

18. Yoshida M, Sasaki M, Sugisaki K, Yamaguchi Y, Yamada M: Neutrophil extracellular trap components in fibrinoid necrosis of the kidney with myeloperoxidase-ANCA-associated vasculitis. Clin Kidney J 2013, 6:308-312.

19. Yang SH, Wu CC, Shih TT, Chen PQ, Lin FH: Three-dimensional culture of human nucleus pulposus cells in fibrin clot: comparisons on cellular proliferation and matrix synthesis with cells in alginate. Artif Organs 2008, 32:70-73.

20. Masuda S, Nakazawa D, Shida H, Miyoshi A, Kusunoki Y, Tomaru U, Ishizu A: NETosis markers: Quest for specific, objective, and quantitative markers. Clin Chim Acta 2016, 459:89-93.

21. Kiernan JA: Does progressive nuclear staining with hemalum (alum hematoxylin) involve DNA, and what is the nature of the dye-chromatin complex? Biotech Histochem 2018, 93:133-148.

22. Ueki S, Tokunaga T, Fujieda S, Honda K, Hirokawa M, Spencer LA, Weller PF: Eosinophil ETosis and DNA Traps: a New Look at Eosinophilic

Inflammation. Curr Allergy Asthma Rep 2016, 16:54.

23. Nakazawa D, Shida H, Kusunoki Y, Miyoshi A, Nishio S, Tomaru U, Atsumi T, Ishizu A: The responses of macrophages in interaction with neutrophils that undergo NETosis. J Autoimmun 2016, 67:19-28.

24. Ramos-Kichik V, Mondragon-Flores R, Mondragon-Castelan M, Gonzalez-Pozos S, Muniz-Hernandez S, Rojas-Espinosa O, Chacon-Salinas R, Estrada-Parra S, Estrada-Garcia I: Neutrophil extracellular traps are induced by *Mycobacterium tuberculosis*. Tuberculosis (Edinb) 2009, 89:29-37.

25. Schreiber A, Rousselle A, Becker JU, von Massenhausen A, Linkermann A, Kettritz R: Necroptosis controls NET generation and mediates complement activation, endothelial damage, and autoimmune vasculitis. Proc Natl Acad Sci USA 2017, 114:E9618-E9625.

Figure legends

Figure 1. Staining of clots for visualization of NETs

FFPE sections of clots of PMA-treated PMNs were subjected to immunofluorescent staining for Cit H3 (**A** and **C**; Red, Cit H3; blue, DAPI employed for DNA staining) and SH staining (**B** and **D**). (**A** and **B**) Before DNase I treatment. (**C** and **D**) After DNase I treatment (10 U/ml, for 1 h, at 37 ºC). Bar, 20 μm.

Figure 2. Presence of NETs in vasculitic lesions

FFPE tissue sections were subjected to HE staining (**A**, **C**, **E**, and **G**) and immunofluorescent staining for Cit H3 and CD15 (**B**, **D**, **F**, and **H**). Red, Cit H3; Green, CD15; Blue, DNA. Bar, 100 μm (**A**, **B**, **E**, and **F**); 200 μm (**C**, **D**, **G**, and **H**). Arrows indicate NETs. (**I**) Area occupied by NETs within the lesion, as determined by image analysis. *$p<0.05$.

Figure 3. Presence of NETs in pulmonary granulomas

FFPE lung sections were subjected to HE staining (**A**, **C**, and **E**) and immunofluorescent staining for Cit H3 and CD15 (**B**, **D**, and **F**). Red, Cit H3; Green, CD15; Blue, DNA. Bar, 100 μm (**A**, **B**, **C**, and **D**); 200 μm (**E** and **F**). Arrows indicate NETs. (**G**) Area occupied by NETs within the lesion, as determined by image analysis. *$p<0.05$, **$p<0.01$.

Figure 4. Disordered degradation of NETs in GPA

FFPE lung sections of GPA and tuberculosis were treated with or without 10 U/ml DNase I for 1 h at 37 ºC. After washing with PBS, the sections were subjected to DAPI staining (**A**, **B**, **E**, and **F**) or SH staining (**C**, **D**, **G**, and **H**). (**A**, **C**, **E**, and **G**) Before

DNase I treatment. (**B**, **D**, **F**, and **H**) After DNase I treatment. Bar, 50 μm. (**I**) Percentage of NETs remaining after DNase I treatment (NETs residual rate), as determined by DAPI staining. *$p<0.05$. (**J**) NETs residual rate, as determined by SH staining. *$p<0.05$.

Legend for Supplemental Figures

Figure S1. Digestion of NETs in necrotizing granulomas of tuberculosis by DNase I. FFPE lung sections of tuberculosis were deparaffinized with xylene and then subjected to antigen retrieval in an autoclave (at 121 ºC for 20 min) with citrate buffer (pH 6.0). Thereafter, the sections were allowed to react with 0 (**Control**; **A**, **B** and **C**) or 10 U/ml DNase I for 1 h at 37 ºC (**D**, **E**, and **F**). After washing with PBS, the sections were subjected to immunofluorescent staining for Cit H3 (red) and CD15 (green) and followed by mounting with a DAPI-containing solution (DNA: blue). A considerable amount of Cit H3 remained after DNase I treatment, whereas DAPI-positive DNA was evidently digested by DNase I. Bar, 50 μm. Representative findings are shown (patient No. 21).

Figure S2. Digestion of NETs in necrotizing vasculitis of MPA by DNase I.

(**A**) The deposition of NETs in necrotizing vasculitis of MPA (red, Cit H3; green, CD15; blue, DNA). FFPE tissue sections of MPA were deparaffinized with xylene and then subjected to antigen retrieval in an autoclave (at 121 ºC for 20 min) with citrate buffer (pH 6.0). Thereafter, the sections were allowed to react with 0 (**B**) or 10 U/ml DNase I for 1 h at 37 ºC (**C**). After washing with PBS, the sections were mounted with DAPI containing solution. The pixel counts in the DAPI-positive areas were 272339 and 264856 in **B** and **C**, respectively. These findings suggest the resistance of NETs in necrotizing vasculitis of MPA to DNase I. Bar, 50 μm. Representative findings are shown (patient No. 3).

Figure 1

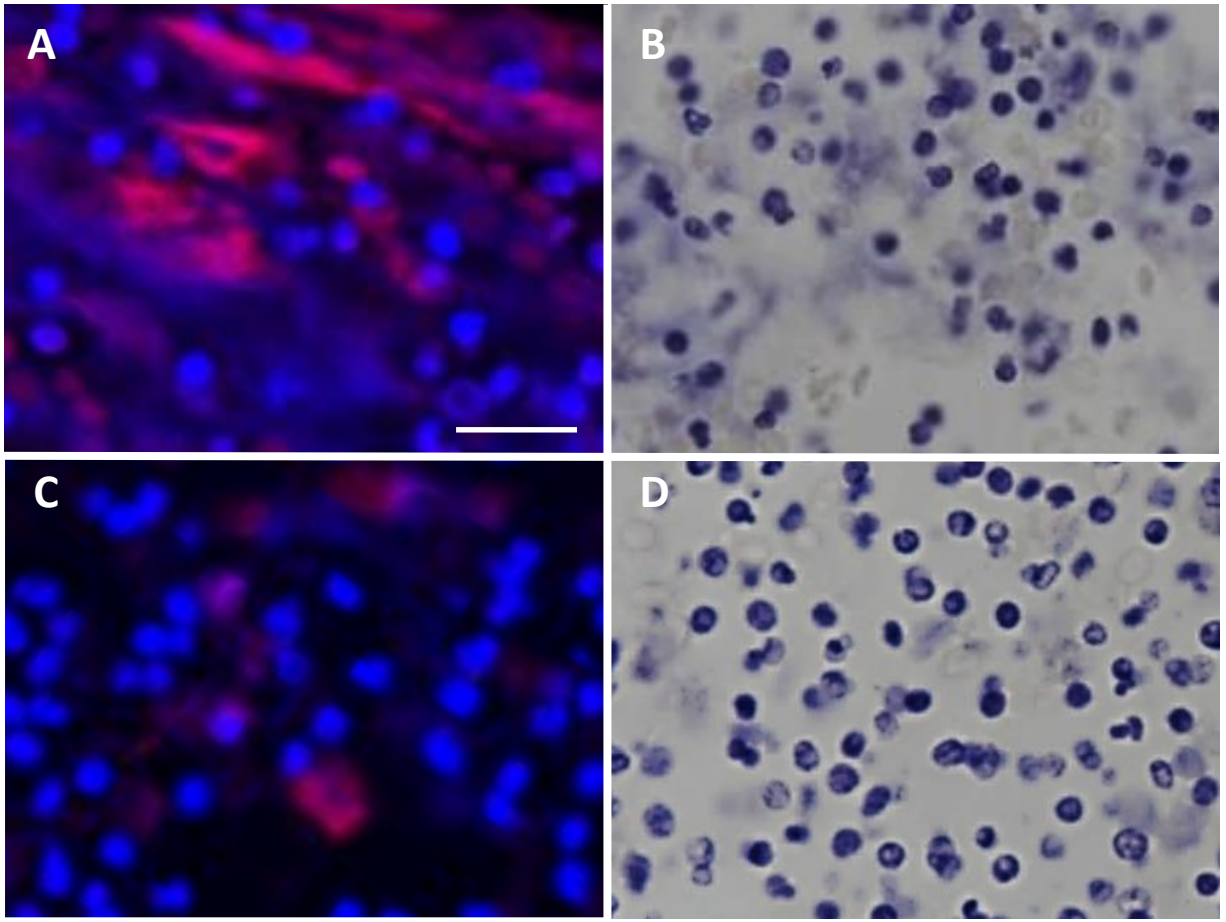

Figure 2

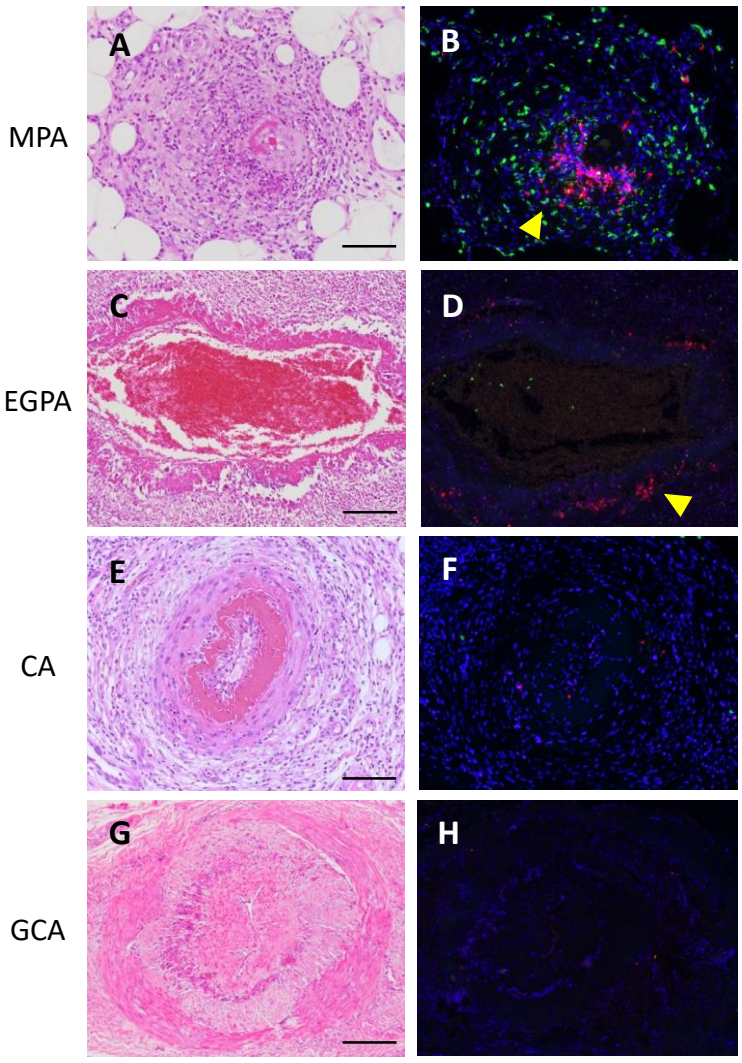
MPA
EGPA
CA
GCA
A
B
C
D
E
F
G
H

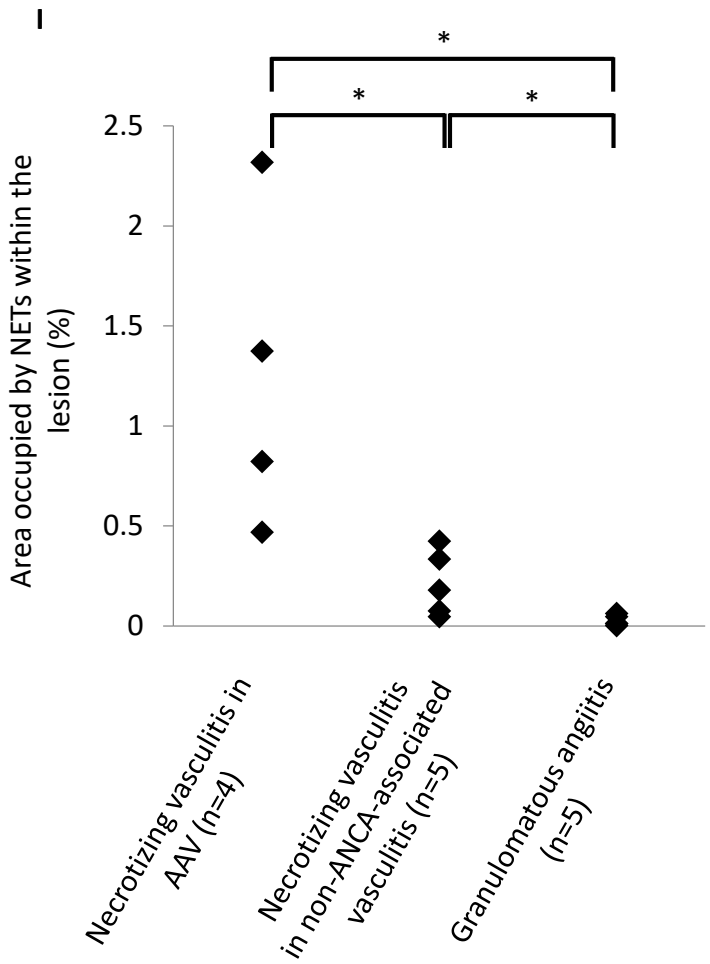
I
Area occupied by NETs within the lesion (%)
2.5
2
1.5
1
0.5
0
*
*
*
Necrotizing vasculitis in AAV (n=4)
Necrotizing vasculitis in non-ANCA-associated vasculitis (n=5)
Granulomatous angiitis (n=5)

Figure 3

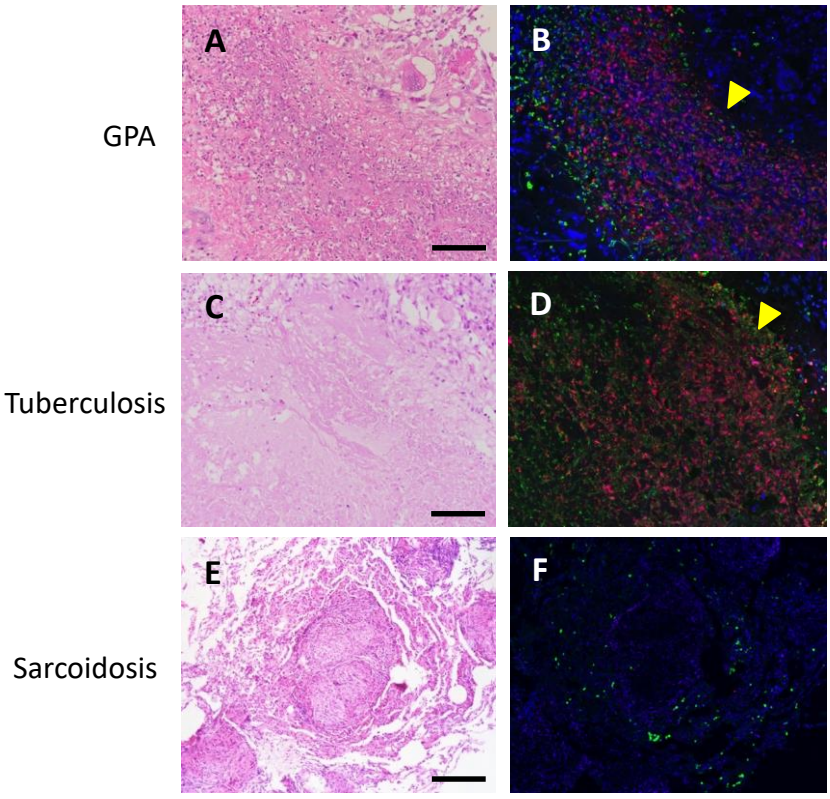
GPA
Tuberculosis
Sarcoidosis
A
B
C
D
E
F

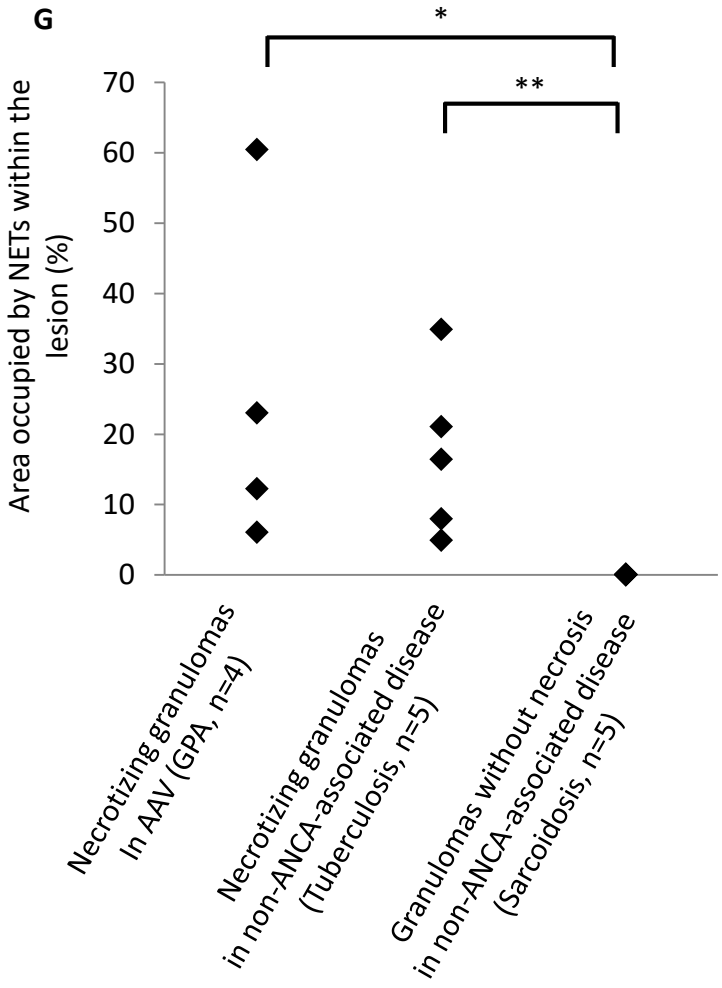
G
*
**
70
60
50
40
30
20
10
0
Area occupied by NETs within the lesion (%)
Necrotizing granulomas In AAV (GPA, n=4)
Necrotizing granulomas in non-ANCA-associated disease (Tuberculosis, n=5)
Granulomas without necrosis in non-ANCA-associated disease (Sarcoidosis, n=5)

Figure 4

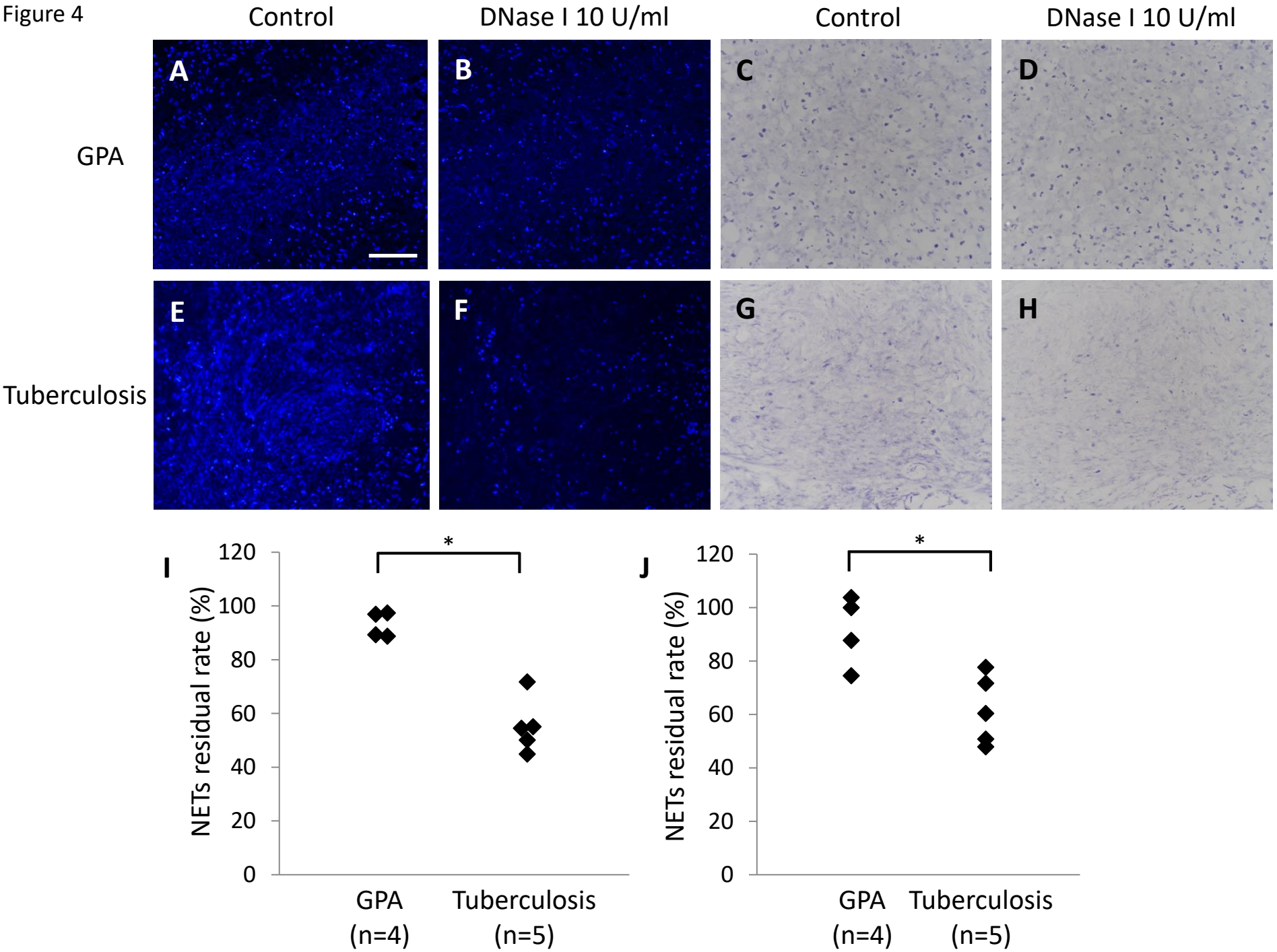
Control
DNase I 10 U/ml
Control
DNase I 10 U/ml
GPA
Tuberculosis
A
B
C
D
E
F
G
H
I
J
NETs residual rate (%)
120
100
80
60
40
20
0
*
GPA
(n=4)
Tuberculosis
(n=5)

Table 1. FFPE specimens used in this study.

Patient No.	Age	Sex	Diagnosis	Tissue obtained	Lesions	Group in Figures 2 and 3
1	71	F	MPA	Muscle biopsy	1	Necrotizing vasculitis in AAV
2	56	M	MPA	Muscle biopsy	4	Necrotizing vasculitis in AAV
3	82	F	MPA	Kidney biopsy	1	Necrotizing vasculitis in AAV
4	61	F	EGPA	Intestine in autopsy	2	Necrotizing vasculitis in AAV
5	66	M	GPA	Lung in autopsy	3	Necrotizing granulomas in AAV
6	58	M	GPA	Lung resection	1	Necrotizing granulomas in AAV
7	37	F	GPA	Lung resection	1	Necrotizing granulomas in AAV
8	49	M	GPA	Lung biopsy	1	Necrotizing granulomas in AAV
9	78	F	PAN	Muscle biopsy	2	Necrotizing vasculitis in non-AAV
10	39	M	PAN	Skin biopsy	1	Necrotizing vasculitis in non-AAV
11	45	F	PAN	Skin biopsy	2	Necrotizing vasculitis in non-AAV
12	27	F	CA	Skin biopsy	1	Necrotizing vasculitis in non-AAV
13	49	F	CA	Skin biopsy	2	Necrotizing vasculitis in non-AAV
14	72	F	GCA	Temporal artery biopsy	1	Granulomatous angiitis
15	72	F	GCA	Temporal artery biopsy	1	Granulomatous angiitis
16	83	F	GCA	Temporal artery biopsy	1	Granulomatous angiitis
17	72	M	GCA	Temporal artery biopsy	1	Granulomatous angiitis
18	71	F	GCA	Temporal artery biopsy	1	Granulomatous angiitis
19	57	M	Tuberculosis	Lung resection	1	Necrotizing granulomas in non-ANCA-associated disease
20	75	M	Tuberculosis	Lung resection	2	Necrotizing granulomas in non-ANCA-associated disease
21	73	F	Tuberculosis	Lung resection	1	Necrotizing granulomas in non-ANCA-associated disease

22	63	M	Tuberculosis	Lung resection	1	Necrotizing granulomas in non-ANCA-associated disease
23	66	M	Tuberculosis	Lung resection	1	Necrotizing granulomas in non-ANCA-associated disease
24	46	F	Sarcoidosis	Lung biopsy	1	Granulomas without necrosis in non-ANCA-associated disease
25	44	M	Sarcoidosis	Lung biopsy	2	Granulomas without necrosis in non-ANCA-associated disease
26	63	F	Sarcoidosis	Lung resection	1	Granulomas without necrosis in non-ANCA-associated disease
27	45	F	Sarcoidosis	Lung resection	1	Granulomas without necrosis in non-ANCA-associated disease
28	36	F	Sarcoidosis	Lung resection	1	Granulomas without necrosis in non-ANCA-associated disease

Table 2. NET deposition in vasculitic lesions

	Necrotizing vasculitis		Granulomatous angiitis (GCA)
	ANCA-associated (MPA, EGPA)	Non-ANCA-associated (PAN, CA)	
NET deposition	+	-	-
Resistance to DNase I	+	Not tested	Not tested

Table 3. NET deposition in necrotizing granulomas

	Necrotizing granulomas		Granulomas
	ANCA-associated (GPA)	Non-ANCA-associated (Tuberculosis)	without necrosis (Sarcoidosis)
NET deposition	+	+	-
Resistance to DNase I	+	-	Not tested